Minimum detectable activity (MDA) for the real-time imaging based on coded-aperture gamma camera

Seoryeong Park, Jihwan Boo, Manhee Jeong*
Jeju National University, 102 Jejudaehak-ro, Jeju-si, Jeju-do, 63243, S. Korea
*Corresponding author: mhjeong@jejunu.ac.kr

1. Introduction

In nuclear security applications, coded-aperture based gamma camera can offer a wealth of spatial information with respect to the mapping of both the radioactive and nonradioactive elements of the objects. Coded-aperture techniques have been successfully applied for arms control and nuclear nonproliferation applications. Compared to Compton cameras, radiographic images using coded-aperture have superior advantages such as angular resolution, measurable energy range, simultaneous multiple nuclide identification, dose linearity, and sensitivity [1]. Based on this, coded-aperture based gamma ray imager development is being actively conducted to shorten the time required for image acquisition. By developing a unique mosaic pattern MURA without using the existing anti-mask method, it was possible to reduce the shooting time by half and reduce the artifact successfully [2]. Traditional coded-aperture-based gamma imaging equipment mainly uses thin lead or tungsten masks. However, Thin masks can ideally carry a pattern projection, but because of their high transmittance, the rays that need to be blocked will pass through the mask, resulting in a high background signal that can damage this signal. On the other hand, thick masks mitigate this phenomenon, but they do not pass through the necessary rays, distorting the shape of the pattern cast into the sensor and creating artifacts. Thickness artifacts are deterministic and do not depend on exposure time or object activity. Therefore, optimal mask thickness is a necessary step in terms of image quality for the real-time gamma ray imaging.

2. Methods and Results

2.1 Method for the optimization of MURA mask thickness

Peak signal-to-noise ratio (PSNR), normalized mean-square error (NMSE), full-width-half maximum (FWHM) and structural similarity (SSIM) are factors used in image quality evaluation of various radiological images. Generally, it is used as an evaluation index of image quality degradation and noise generation in reconstructed images at the time of image reconstruction. If the PSNR is 30 dB or more, it is judged that the reconstructed image is of good quality, which is hard to distinguish from the original image [3]. The PSNR can be calculated by the following equation (1) [4].

$$PSNR(f,g) = 10log_{10}\left(\frac{255^2}{MSE(f,g)}\right) \quad (1)$$

where MSE is mean square error when f and g are reference image and reconstructed image for grey-level (8 bits) images, respectively. The MSE can be calculated when the image size is M x N by the following equation (2)

$$MSE(f,g) = \frac{1}{MN}\sum_{i=1}^{M}\sum_{j=1}^{N}\left(f_{ij} - g_{ij}\right)^2 \quad (2)$$

If there is no difference between the original image and the NMSE, the value becomes 0. If the NMSE is closer to 0, it is regarded as no difference from the original image. The NMSE can be calculated by the following equation (3) [4].

$$NMSE = \frac{\sum_{i=1}^{M-1}\sum_{j=1}^{N-1}(f_{ij}-g_{ij})^2}{\sum_{i=1}^{M-1}\sum_{j=1}^{N-1}(f_{ij})^2} \quad (3)$$

FWHM is also used as an index to evaluate spatial resolution. Spatial resolution is an important factor in evaluating the performance of a device or in controlling quality [9]. In addition, the SSIM is also used as an index to evaluate structural similarity. If there is no structural difference from the original image, the value becomes 1, and when it is close to 1, it is considered that there is no structural difference from the original image [10]. The SSIM can be calculated by the following equation (4) when w are 11 x 11 circular-symmetric Gaussian weighting function $w = \{w_i \mid i = 1,2,\cdots,N\}$ with standard deviation of 1.5 samples, normalized to unit sum $(\sum_{i=1}^{N} w_i = 1)$ [5].

$$SSIM(f,g) = \frac{(2\mu_f\mu_g+C_1)(2\sigma_{fg}+C_2)}{\left(\mu_f^2+\mu_g^2+C_1\right)\left(\sigma_f^2+\sigma_g^2+C_2\right)} \quad (4)$$

where μ_f, μ_g, σ_f, σ_g, and σ_{fg} are mean luminance and unbiased estimate in discrete form for the images of f and g, and C_1 and C_2 are used to avoid a null denominator.

Therefore, the values of PSNR, NMSE, FWHM, and SSIM for the Monte Carlo simulated and reconstructed images were performed to optimize the thickness of the aperture.

2.2 MURA mask thickness optimization

In Figure 1(a), both CC and MLEM methods have a maximum at around 2 to 5 cm. However, the CC method

has a maximum value of about 25 ~ 30 dB depending on the source energy, and the MLEM technique has a maximum value of about 175 ~ 255 dB depending on the source energy. Therefore, it can be seen that the same image as the original image can be obtained when the thickness of the mask is 2 to 5 cm in terms of PSNR.

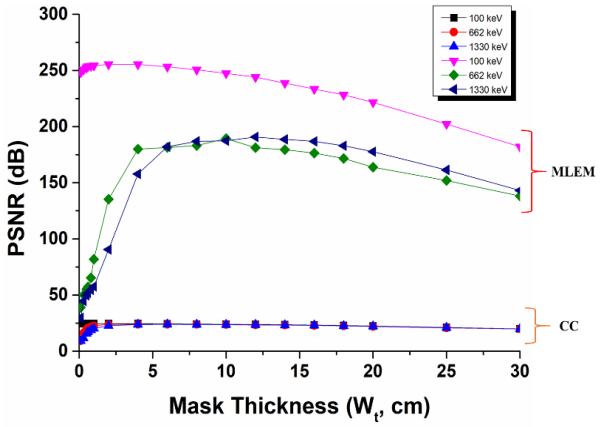

(a)

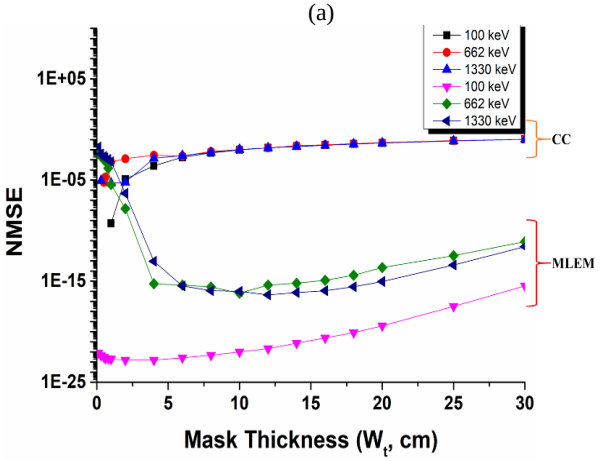

(b)

Fig. 1. Variation of PSNR (a) and NMSE (b) by Gamma ray energy and image reconstruction techniques for increasing mask thickness.

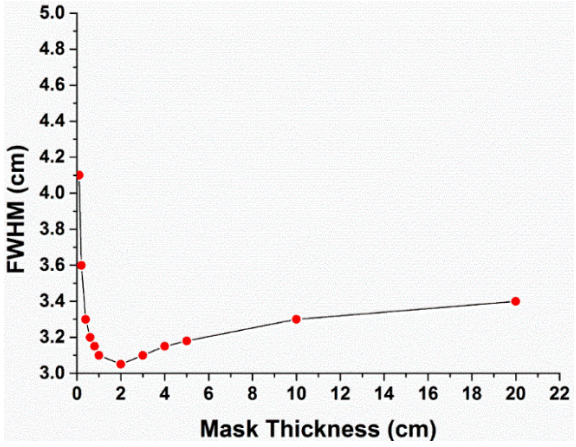

Fig. 2. Graph of the FWHM versus increasing mask thickness.

In Fig. 1(b), the correlation method has a minimum value in the vicinity of 1 x 10^{-8} ~ 1 x 10^{-5} according to the energy of the source when the tungsten thickness is 0 ~ 2.5 cm, and the repetitive image reconstruction technique has a minimum value in the vicinity of 1 x 10^{-23} ~ 1 x 10^{-14} depending on the energy of the source when the tungsten thickness is 2 ~ 4 cm. Therefore, when the thickness of the mask is 2 ~ 4 cm in terms of NMSE, the difference from the original image is the least. It is generally considered that the smaller the FWHM, the better the spatial resolution. In Fig. 2, it can be seen that FWHM has the minimum value in the vicinity of 2 cm. Therefore, it can be seen that the spatial resolution is the best when the spatial resolution is 2 cm.

In Fig. 3, the maximum value of SSIM is about 1 ~ 16 cm in the MLEM method, and the maximum value is about 0.9994 ~ 0.9999 in the CC method about 0.6 ~ 2 cm. Therefore, it can be seen that when the thickness of the mask is about 2 cm in terms of SSIM, the difference from the original image is the least. Considering the results of the above four factors (PSNR, NMSE, FWHM, SSIM), which are used as an index to evaluate the radiological image, and the cost aspect, in this study, 2 cm is the most optimal mask thickness.

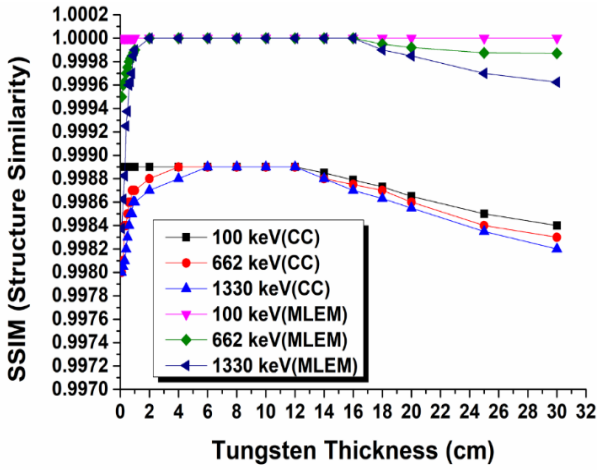

Fig. 3. Image reconstruction using MLEM for 662 keV point, line, and surface sources based on Monte Carlo simulation.

2.3 Derive minimum detection dose for real-time image acquisition

As shown in Fig. 4a, both the correlation method and the repetitive image reconstruction technique have an increase in PSNR as the number of incident radiation increases. As mentioned in the previous section 2.1, the PSNR is considered to be 30 dB or more, and the MLEM is 30 dB when the incident radiation is about 100 cps. However, we confirmed that PSNR values are less than 30 dB in image reconstruction using correlation technique. Also, as shown in Fig. 4b, it can be seen that the NMSE value decreases gradually as the number of incident radiation increases in both methods. As mentioned in Section 2.1, the NMSE is considered to be

smaller than the original image, and the iterative image reconstruction method converges to 0.1 when the radiation count is more than about 1000 cps.

Also, as shown in Fig. 5, it can be seen that the SSIM value increases gradually as the number of incident radiation increases in both methods.

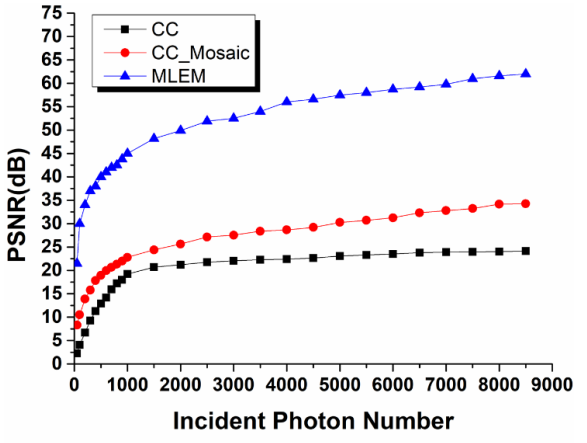

(a)

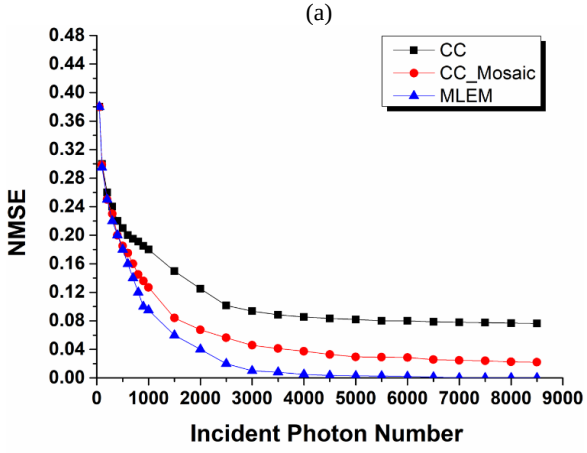

(b)

Fig. 4. Graph of (a) PSNR and (b) NMSE according to increasing incident photon number.

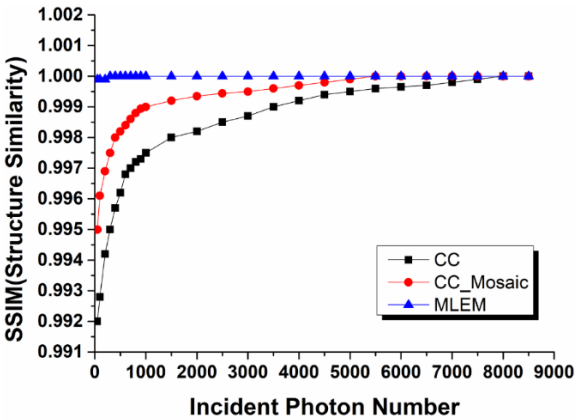

Fig. 5. Graph of SSIM according to increasing incident photon number.

In addition, the SSIM is considered to be less structurally different from the original image. The iterative image reconstruction technique converges to 1 when the incident radiation number is more than 1000 cps. Therefore, in this study, 1000 cps was judged optimal for the minimum detectable dose. That is, the minimum detected count rate is about 5.04875 x 10^6 Bq (0.13645 mCi) at 1 meter source-to-detector distance.

4. Conclusion

In this study, computational simulation using MCNPX-Polimi was performed to derive the minimum detectable counts for real-time imaging of coded aperture radiographic imaging equipment. It is confirmed that the optimum image is reconstructed when the thickness of the mask is ~2 cm. Also, it was confirmed that the image was reconstructed irrespective of the shape of the source by changing the number of ranks. And that the minimum detectable count for the real-time imaging of the coded-aperture gamma camera is ~1000 cps.

Estimation of the minimum detection counts for real-time imaging can be used in the design of gamma ray cameras, which can be used in radiation imaging for the nuclear power plants such as operation, protection of radiation workers, and decommissioning and decontamination.

REFERENCES

[1] R. Accorsi, Design of near-field coded aperture camera for high resolution medical and industrial gamma-Ray imaging, Ph.D. thesis Massachusetts Institute of Technology. Dept. of Nuclear Engineering, 2001.

[2] M. Jeong, M.D. Hammig, “Comparison of gamma ray localization using system matrixes obtained by either MCNP simulations or ray-driven calculations for a coded-aperture imaging system,” Nuclear Instruments and Methods in Physics Research Section A: Accelerators, Spectrometers, Detectors and Associated Equipment, vol. 893, In Press, 2018.

[3] R. Chaves, J.Ramírez, J.M.Górriz, M.López, D.Salas-Gonzalez, I.Álvarez, F.Segovia, SVM-based computer-aided diagnosis of the Alzheimer's disease using t-test NMSE feature selection with feature correlation weighting, Neuroscience Letters, vol. 461, pp. 293-297, 2009.

[4] A. Hore, D. Ziou, “Image Quality Metrics: PSNR vs. SSIM,” Proc. ICPR, vol. 34, pp. 2366-2367, 2010.

[5] P. Ndajah, H. Kikuchi, M. Yukawa, H. Watanabe, and S. Muramatsu, "SSIM Image Quality Metric for Denoised Images," in WSEAS International conference on Visualization, Imaging and Simulation, pp. 53-57, Nov. 2010.